Environment, Climate Change and Low Carbon Economy Programme

'Environment Programme'

European Economic Area (EEA) Financial Mechanism 2014-2021

A2 Report – Characterisation of waste

15/12/2021

37_Call#2_Circular Construction in Energy-Efficient Modular Buildings

Accordingly, with the Articles 25.2.j) and 29.4 of the 'Applicants Guide for Financing of Projects Supported by Environment, Climate Change and Low Carbon Economy Programme'
https://www.eeagrants.gov.pt/media/2994/applicants-guide-for-financing-eea-grants_environment-projects_28112019.pdf

1. Introduction

This report presents the actions developed during the activity A2 (Characterization of Wastes), which were concluded by the end of November 2021. It also explains some slight deviations to the original planning, related with the inclusion of more wastes than initially defined.

The University of Trás-os-Montes and Alto Douro (UTAD) was originally targeting five wastes, due to the previous experience of the team with these wastes. Subsequently, three additional wastes were added, after the start of the project. The Faculty of Sciences of the University of Porto (FCUP) focused on the collection, storage, and characterization of one residue. Moreover, an additional glass waste was added to the list, as a possible substitute of the original glass waste. The total list of wastes characterized and tested in Activity 2 are:

1. Polyurethane ;
2. Timber ;
3. Incinerated Municipal Solid Waste slag;
4. Optical lenses glass;
5. Bottle glass;
6. Ceramic;
7. Plastic;

8. Coal Fly Ash;
9. Marble cutting;
10. Granite cutting;

2. Characterization

2.1. Polyurethane

This waste was only submitted to the particle size and morphology analysis, using sieving and scanning electron microscopy, since its particular properties were either not suitable for the majority of the tests performed on most of the remaining wastes, or its nature didn't require some of those tests (e.g. it is an inert material and, this, an environmental analysis, through leaching recovering, was deemed unnecessary). Furthermore, although this waste is useful, as it contributes for the development of a highly porous composite material, it does not, in itself, possess the structural integrity required for a mechanical strength test.

2.1.1. Particle size distribution

The polyurethane residue was provided in a range of granulometries, and was standardized using a 1,60mm sieve. Figure 1 shows the result on the material after the sieving.

Figure 1 - Standardization of material before (a) and after (b) sieving

2.1.2. Morphology (Scanning Electron Microscopy)

The microstructure of this residue is presented in Figure 2, obtained from scanning electron microscopy.

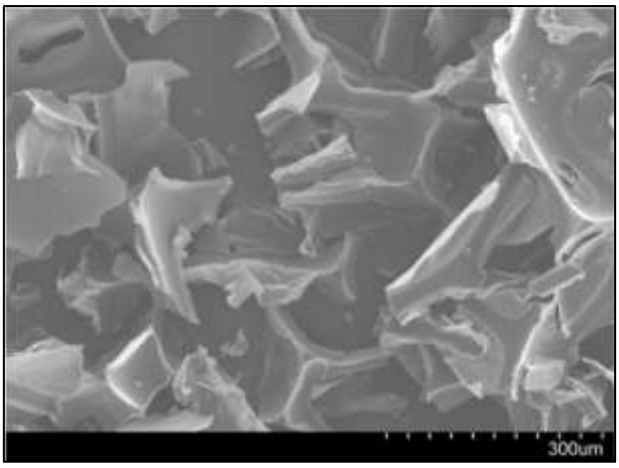

Figure 2 - Microstructure of polyurethane residue

2.2. Timber residue

This waste was only submitted to the particle size and density analysis, since its particular properties were either not suitable for the majority of the tests performed on most of the remaining wastes, or its nature didn't require some of those tests (e.g. it is an inert material and, this, an environmental analysis, through leaching recovering, was deemed unnecessary). Furthermore, although this waste is useful, as it contributes for the development of a highly porous composite material, it does not, in itself, possess the structural integrity required for a mechanical strength test.

2.2.1. Density

The timber residue is composed in its majority of Pinus Pinaster. The density of the residue was obtained through the ISO 17892-3, and the results are presented in Table 1.

Table 1 - Timber residue density

Sample		1	2	3
Weight of pycnometer (m_1)	(g)	14,90	19,52	17,39
Weight of pycnometer + soil (m_2)	(g)	16,91	21,52	19,39
Weight of pycnometer + soil + water (m_3)	(g)	73,17	76,23	75,29
Weight of pycnometer + water (m_4)	(g)	72,45	75,66	74,70

Weight of soil (m_2-m_1)	(g)	2,01	1,99	2,00
Weight of water with full pycnometer (m_4-m_1)	(g)	57,55	56,13	57,31
Weight of water (m_3-m_2)	(g)	56,27	54,72	55,90
Volume of soil	(ml)	1,29	1,42	1,41
Density of particles	(KN/m^3)	15,31	13,80	13,91
Density	(KN/m^3)	14,34		

2.2.2. Particle size distribution

The particle size distribution of the material was determined by sieving, according to ISO 17892-4. Only the material with granulometry higher than 63µm was used. Figure 3 presents the granulometric curve.

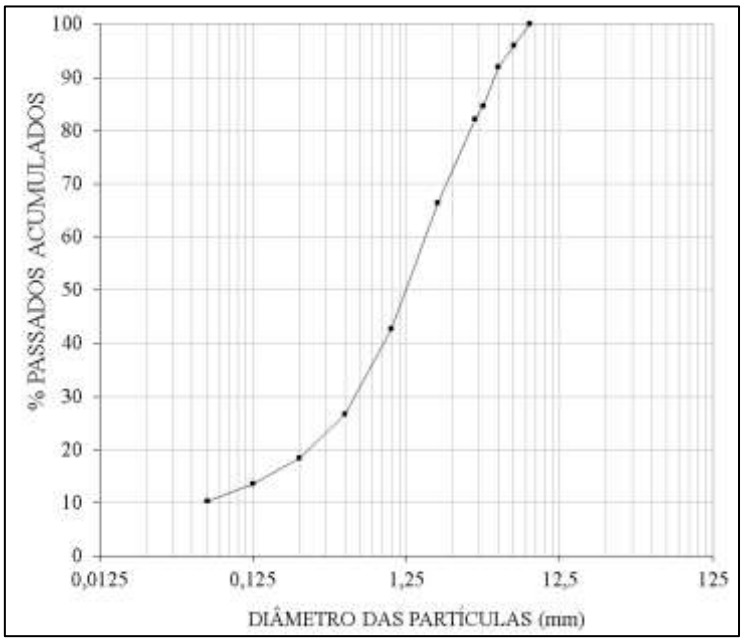

Figure 3 – Timber residue granulometry

2.3. Slag

2.3.1. Particle size distribution

The slag, obtained from the LIPOR company, was provided with a granulometry smaller than 2,0mm, after hand-removal of bigger materials. Initial treatment was needed using the Los

Angeles abrasion equipment. Approximately 20kg of material and 15kg of steel spheres were used, and the granulometry was checked by weighting the total amount of retained material on the 63µm and 50µm sieves, after each milling cycle. The weights are presented on Table 2, and a more precise granulometry of the material is shown in Figure 4. Figures 5 and 6 show the material retained by each sieve before and after the final milling cycle,

Table 2 – Retained material after each milling cycle

Passing after 0h	63 µm	5,17 g	5,17%
	50 µm	3,30 g	3,28%
Passing after 16h	63 µm	47,50 g	51,91%
	50 µm	43,60 g	43,00%
Passing after 26h	63 µm	57,96 g	57,93%
	50 µm	52,8 g	52,59%
Passing after 36h	63 µm	68,78 g	68,59%
	50 µm	63,65 g	63,55%

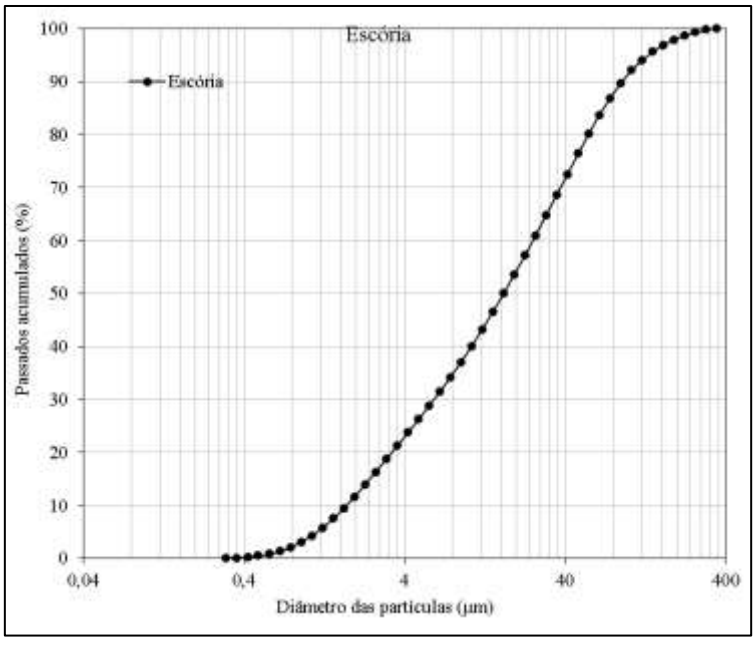

Figure 4 – LIPOR slag granulometry

Figure 5 – Passing material at 0h

Figure 6 - Passing material after 36h

2.3.2. Composition

Table 3 and Figure 7 show the results of the EDS analysis and the X-Ray, respectively. Figure 8 shows the SEM analysis of the material.

Table 3 - EDS results

Element	Wt %	At %	K-Ratio	Z	A	F
NaK	7.00	9.25	0.0187	0.9877	0.2686	10.062
MgK	5.11	6.38	0.0151	10.136	0.2886	10.102
AlK	6.81	7.66	0.0217	0.9848	0.3181	10.159
SiK	43.75	47.31	0.1462	10.144	0.3280	10.042
P K	3.91	3.83	0.0063	0.9816	0.1639	10.049
S K	2.43	2.30	0.0047	10.079	0.1901	10.069
ClK	2.42	2.08	0.0053	0.9654	0.2241	10.096
K	3.12	2.42	0.0100	0.9676	0.3240	10.202
CaK	22.77	17.26	0.0836	0.9900	0.3705	10.010
TiK	0.65	0.41	0.0021	0.9076	0.3502	10.011
FeK	2.03	1.11	0.0121	0.9130	0.6512	10.000
Total	100.00	100.00				

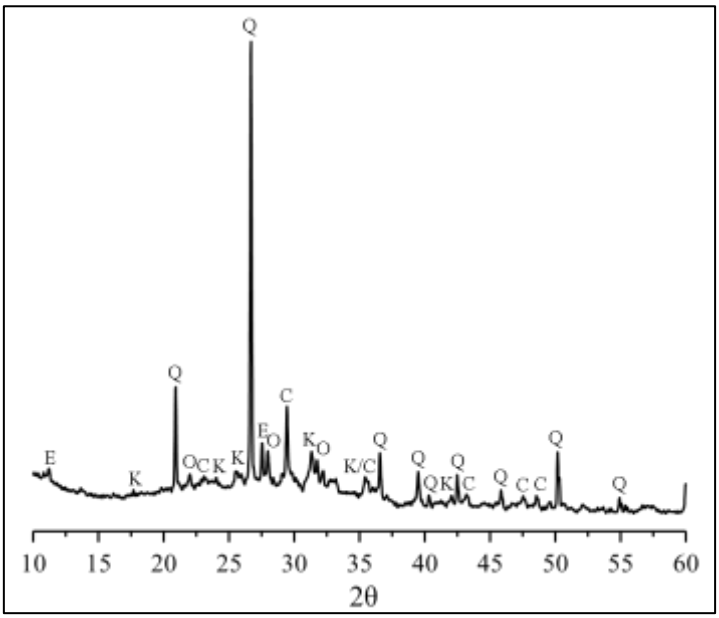

Figure 7 – XRD results

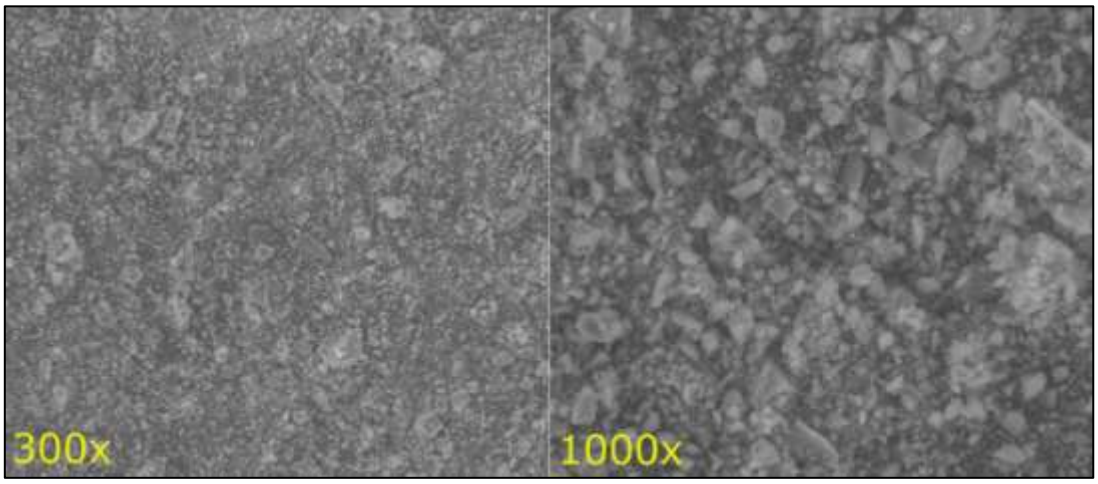

Figure 8 - SEM results

2.3.3. FTIR

Figure 9 shows the results of FTIR analysis using a Shimadzu IRAffinity-1S equipment with wave range between 400 e 4000 cm^{-1}, resolution of 4 and 64 scans.

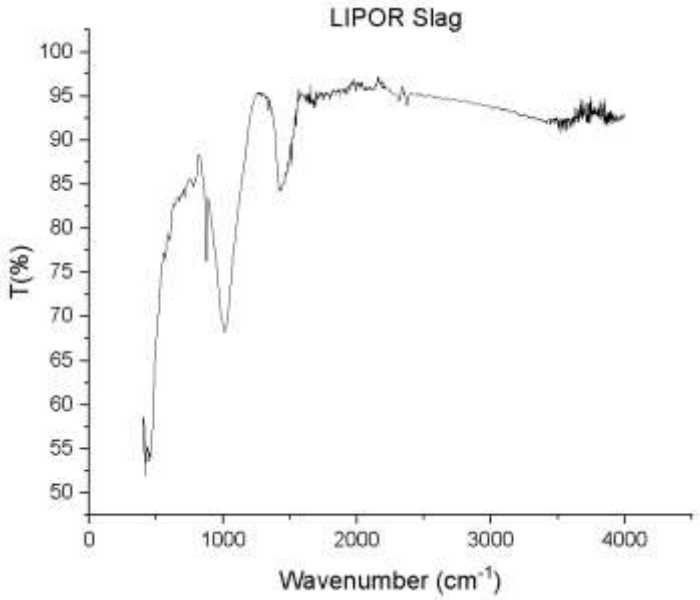

Figure 9 – FTIR analysis

2.3.4. Mechanical Behavior

A single cylindrical specimen was produced to assess the mechanical resistance of the material. The quantity of material used for the paste is presented in Table 4. The activator used was

hydroxide with a molar concentration of 5. The curing process of the paste is presented in Table 5. As shown in Figure 10, the specimen couldn't be unmolded, since it wasn't strong enough. Therefore, there is no mechanical resistance results for this material.

Table 4 – Paste quantities

Residue	Quantity (g)		S/L Ratio
	Precursor	Activator	
LIPOR Slag	100	60	0,60

Table 5 – Curing properties

Residue	Oven			Shelf		
	Temperature (°C)	Humidity (%)	Time (h)	Temperature (°C)	Humidity (%)	Time (h)
LIPOR SLAG	80	0	47	-	-	-

Figure 10 - LIPOR slag specimen (after unmolding)

2.3.5. Leaching results

The leaching tests were conducted according to EN 12457-4. The results of the chemical analysis are as shown in Table 6.

Table 6 – Slag leaching results

Element	Concentration (ppm)	Landfill limit values (ppm)		
		Inert	Non-hazardous	Hazardous
Cu	0,62±0,14	2	50	100
Zn	0,05±0,04	4	50	200
Pb	0,00±0,19	0,5	10	70
Cr	0,00±0,10	0,5	10	50
Chloride	17,58±1,72	800	15000	25000
Sulfate	83,65±6,05	1000	20000	50000

2.4. Lens glass residue

2.4.1. Particle size distribution

The granulometry of the material is presented in Figure 11, and was obtained using laser diffraction, with resolution ranging from 0,9μm to 175μm.

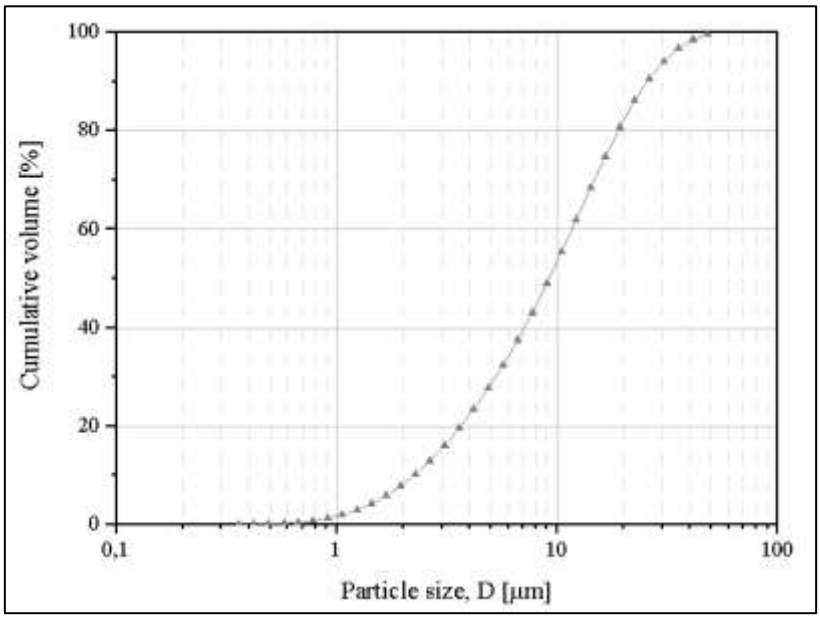

Figure 11 - Glass residue granulometry

2.4.2. Composition

The diffraction pattern obtained from XRD is present in Figure 12. The composition was obtained using XRF and is presented in Table 7.

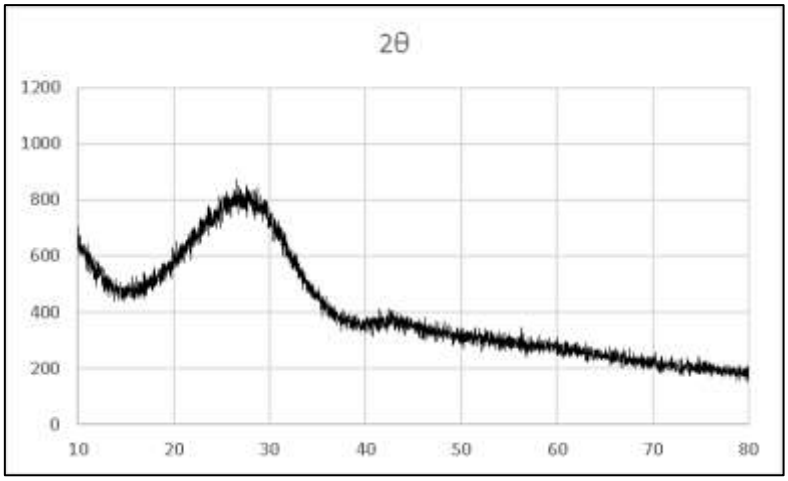

Figure 12 – XRD results

Table 7 - Glass residue composition

Tipo	Element	GP
Chemical composition XRF	Na2O	8,750
	SiO2	58,37
	Al2O3	3,940
	MgO	0,492
	K2O	4,659
	CaO	6,128
	TiO2	2,730
	Fe2O3	0,148
	ZnO	2,572
	ZrO2	2,155
	BaO	2,300
	PbO	5,072
	Others	0,833
	aL.o.I.	1,849
	Si/Al	14,81
Chemical attack 1% HF	Reactive SiO2	42,25 ± 0,27
	Reactive Al2O3	3,52 ± 0,07
	Reactive SiO2 þ Al2O3	45,77
	Reactive SiO2/Al2O3	12,00 ± 0,17

2.4.3. FTIR

Figure 13 presents the FTIR analysis of the glass residue using a Shimadzu IRAffinity-1S equipment with a wave range between 400 e 4000 cm^{-1}, resolution of 4 and 64 scans.

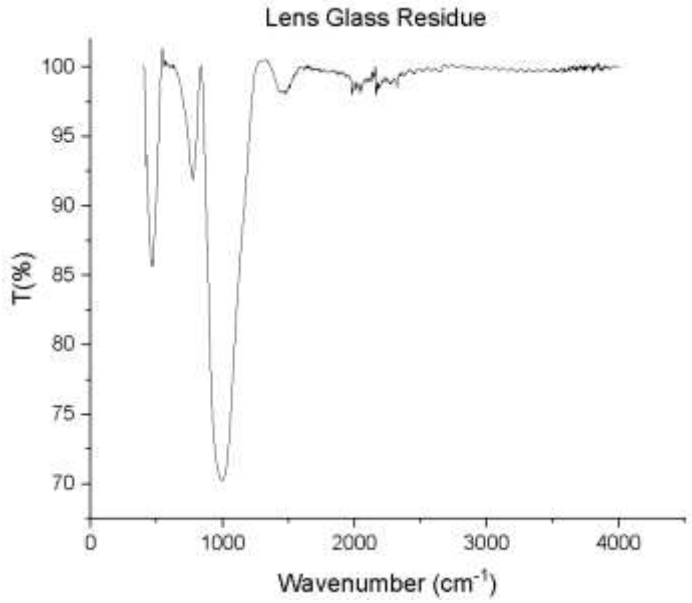

Figure 13 – FTIR results

2.4.4. Mechanical behavior

A single cylindrical specimen was produced to assess the mechanical resistance of the material. The quantity of material used for the paste is presented in Table 8. The activator used was hydroxide with a molar concentration of 5. The curing process of the paste is presented in Table 9. As shown in Figure 14, the specimen couldn't be unmolded, since it wasn't strong enough. Therefore, there is no mechanical resistance results for this material.

Table 8 – Paste quantities

Residue	Quantity (g)		S/L Ratio
	Precursor	Activator	
Lens Glass Residue	80	35	0,44

Table 9 – Curing properties

Residue	Oven			Shelf		
	Temperature (°C)	Humidity (%)	Time (h)	Temperature (°C)	Humidity (%)	Time (h)
Lens Glass Residue	80	0	47	-	-	-

Figure 14 – Lens glass residue specimen (after unmolding)

2.4.5. Leaching results

The leaching tests were conducted according to EN 12457-4. The results are shown in Table 10.

Table 10 – Lens glass residue

Element	Concentration (ppm)	Landfill limit values (ppm)		
		Inert	Non-hazardous	Hazardous
Cu	0,28±0,14	2	50	100
Zn	1,59±0,04	4	50	200
Pb	7,84±0,27	0,5	10	70
Cr	0,02±0,09	0,5	10	50
Chloride	13,37±1,67	800	15000	25000
Sulfate	11,02±3,34	1000	20000	50000

2.5. BAGLASS glass residue

The glass was provided in pieces, with dimensions between 5 and 10 mm, and several colors. The milling was performed on a Retsch S100 mill and a rotation of 580RPM. After the milling, the material was passed through a 500 μm sieve and analyzed. Figure 15 presents the material before and after the initial treatment. This residue shows a better reactivity with the activators; hence it is a possible substitute for the lens glass.

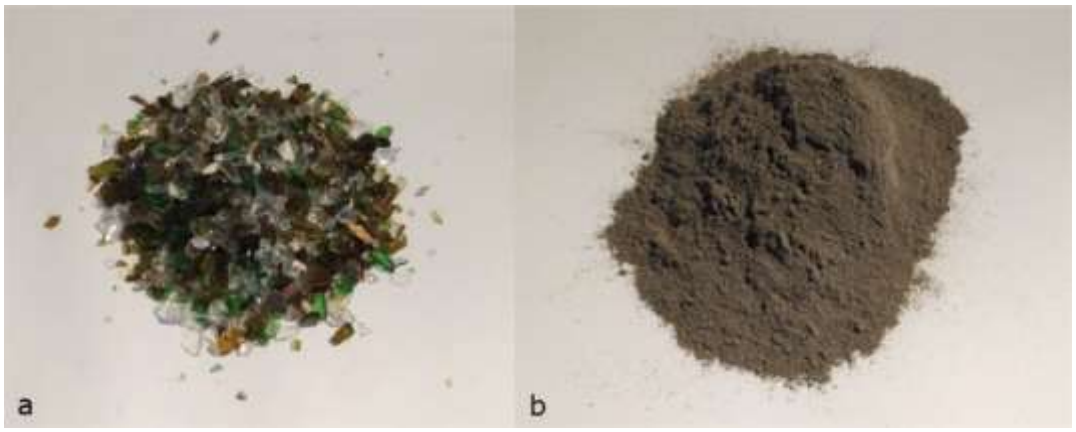

Figure 15 - Pre-treatment of BAGLASS glass

2.5.1. Composition

The XRF analysis is presented in Table 11. The XRD analysis is presented in Figure 16.

Table 11 – XRF analysis of BAGLASS glass

Na2O	MgO	Al2O3	SiO2	P2O5	SO3	Cl
59,8 KCps	14,2 KCps	19,9 KCps	582,2 KCps	0,3 KCps	2,2 KCps	0,8 KCps
12,28	1,31	2,39	68,27	0,051	0,189	0,0449

K2O	MnO	CuO	Cr2O3	Rb2O	Fe2O3	CO2
17,0 KCps	2,7 KCps	3,3 KCps	4,1 KCps	2,5 KCps	68,7 KCps	
0,791	0,0353	0,0129	0,0925	0,002	0,6924	1,43

CaO	TiO2	ZnO	SrO	ZrO2	BaO	PbO
239,8 KCps	2,0 KCps	13,3 KCps	18,5 KCps	21,4 KCps	0,5 KCps	16,5 KCps
12,10	0,112	0,0411	0,0186	0,0179	0,056	0,0578

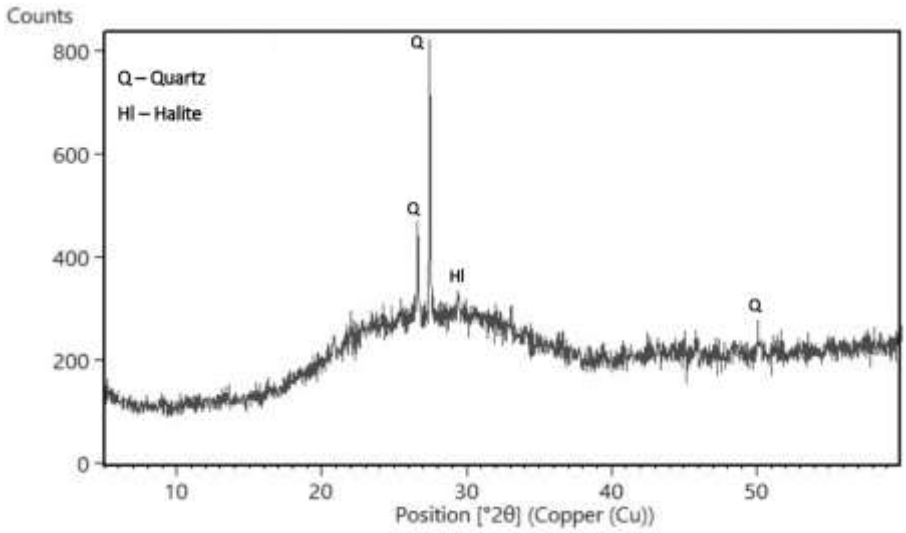

Figure 16 – XRD analysis of BAGLASS glass

2.5.2. FTIR

Figure 17 presents the FTIR analysis of the glass using a Shimadzu IRAffinity-1S equipment with wave range between 400 and 4000 cm^{-1}, resolution of 4 and 64 scans.

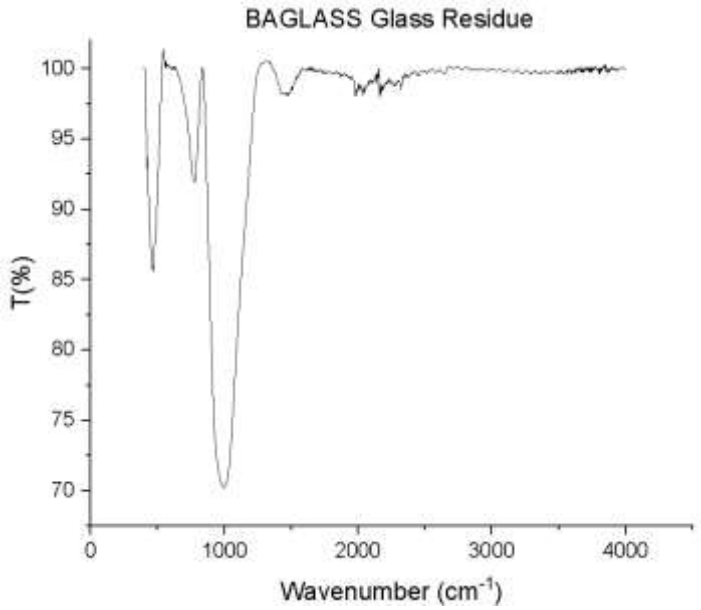

Figure 17 – FTIR analysis of BAGLASS glass

2.5.3. Mechanical behavior

A single cylindrical specimen was produced to assess the mechanical resistance of the material. The quantity of material used for the paste is presented in Table 12. The activator used was hydroxide with a molar concentration of 5. The curing process of the paste is presented in Table 13. The specimen was successfully unmolded, has shown in Figure 18, and the mechanical results are presented in Table 14.

Table 12 – Paste quantities

Residue	Quantity (g)		S/L Ratio
	Precursor	Activator	
BAGLASS Glass Residue	100	50	0,50

Table 13 – Curing properties

Residue	Oven			Shelf		
	Temperature (°C)	Humidity (%)	Time (h)	Temperature (°C)	Humidity (%)	Time (h)
BAGLASS Glass Residue	80	0	47	20	60	48

Figure 18 – BAGLASS glass residue specimen (after unmolding)

Table 14 – Mechanical results

Residue	Mechanical results	
	Compression (kN)	Compression (MPa)
BAGLASS Glass Residue	1,28	1,44

2.5.4. Leaching results

The leaching tests were conducted according to EN 12457-4. The results are as shown in Table 15.

Table 15 – BAGLASS leaching results

Element	Concentration (ppm)	Limit values (ppm)		
		Inert	Non-hazardous	Hazardous
Cu	0,03±0,14	2	50	100
Zn	0,10±0,04	4	50	200
Pb	0,00±0,19	0,5	10	70
Cr	0,00±0,10	0,5	10	50
Chloride	13,55±1,67	800	15000	25000
Sulfate	56,76±4,40	1000	20000	50000

2.6. Ceramic residue

Thanks to its initial disperse granulometry and the presence of bigger particles, the ceramic residue needed to be milled for 32h, using a Los Angeles abrasion equipment to achieve a more usable granulometry. The results here presented are relative to the treated material.

2.6.1. Particle size distribution

The granulometry of the residue is presented in Figure 19, obtained through laser, with resolution between 0,9µm and 175µm.

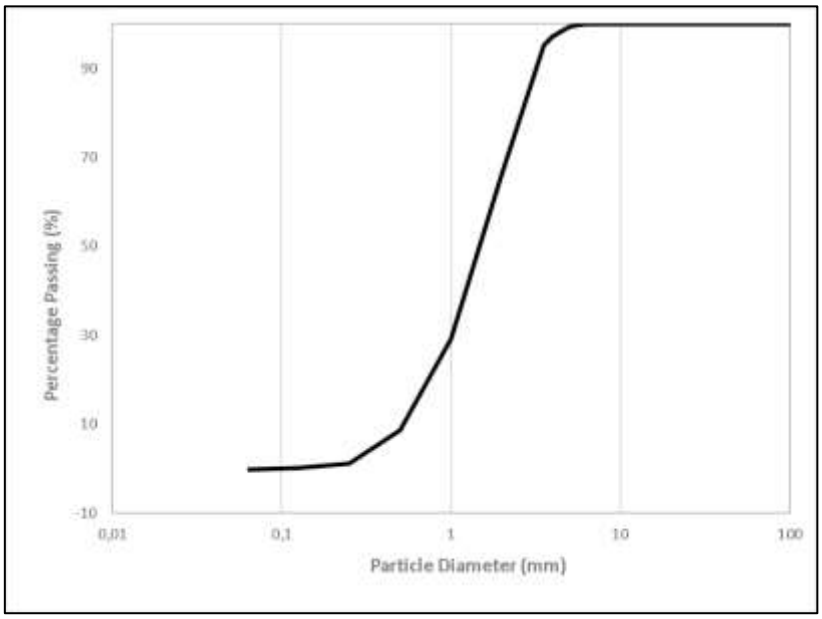

Figure 19 - Ceramic residue granulometry

2.6.2. Composition

The chemical composition of the residue was determined through XRF, presented on Table 16. The diffractogram obtained from XRD analysis is shown in Figure 20.

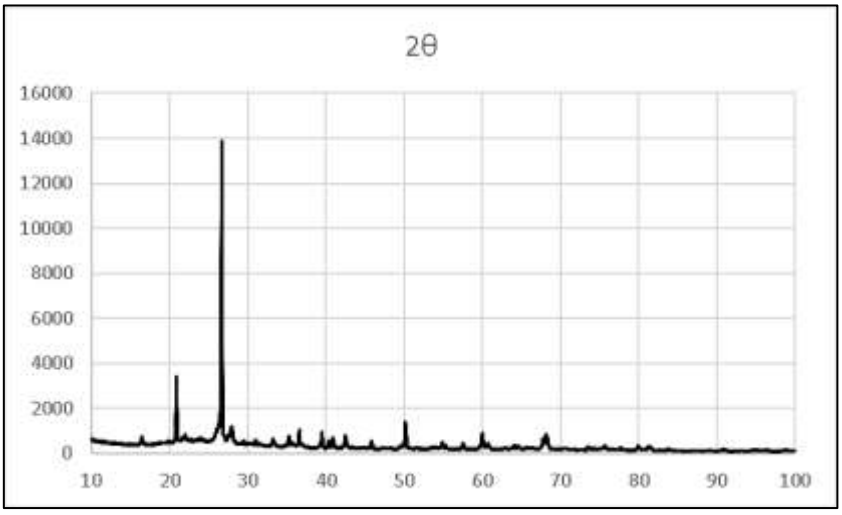

Figure 20 - XRD spectrum

Table 16 - Chemical composition

Material	Al2O3	CaO	Fe2O3	K2O	MgO	Na2O	SiO2	TiO2
(%)	17,87	3,72	1,20	3,18	1,31	1,27	70,98	0,47

Table 17 presents the results of EDS analysis. Figure 21 presents the SEM analysis with magnification from 300 to 2000 times.

Table 17 - EDS analysis

Elem	Wt %	At %	K-Ratio	Z	A	F
NaK	1,85	2,32	0,0065	0,9845	0,351	1,0096
MgK	1,56	1,85	0,0069	1,0103	0,4335	1,0182
AlK	18,62	19,91	0,0979	0,9815	0,524	1,0226
SiK	65,33	67,12	0,2139	1,0111	0,3235	1,001
K K	5,2	3,84	0,0143	0,9631	0,2838	1,0046
CaK	5,23	3,77	0,0163	0,9854	0,3154	1,0008
TiK	0,56	0,34	0,0021	0,9038	0,4218	1,001
FeK	1,65	0,85	0,0112	0,9094	0,7433	1
Total	100	100				

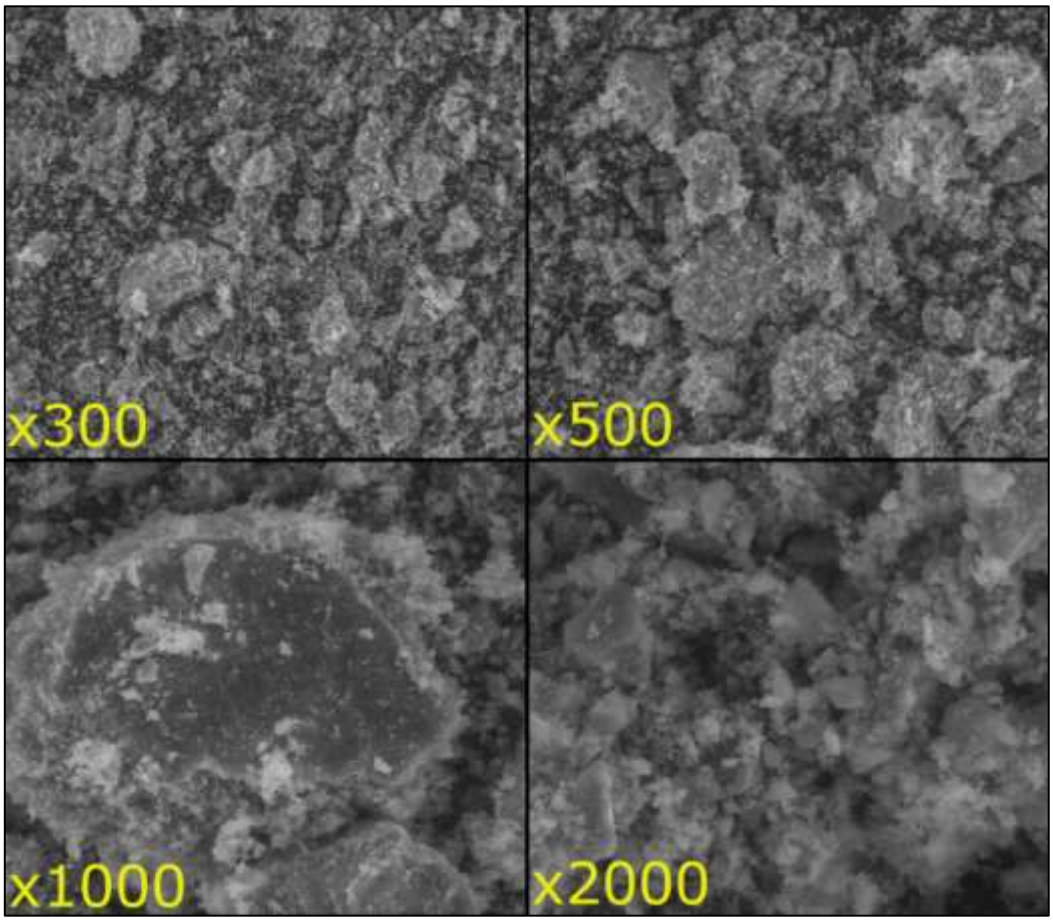

Figure 21 - SEM analysis

2.6.3. FTIR

Figure 22 presents the FTIR analysis of the ceramic residue using a Shimadzu IRAffinity-1S equipment with wave range between 400 and 4000 cm^{-1}, resolution of 4 and 64 scans.

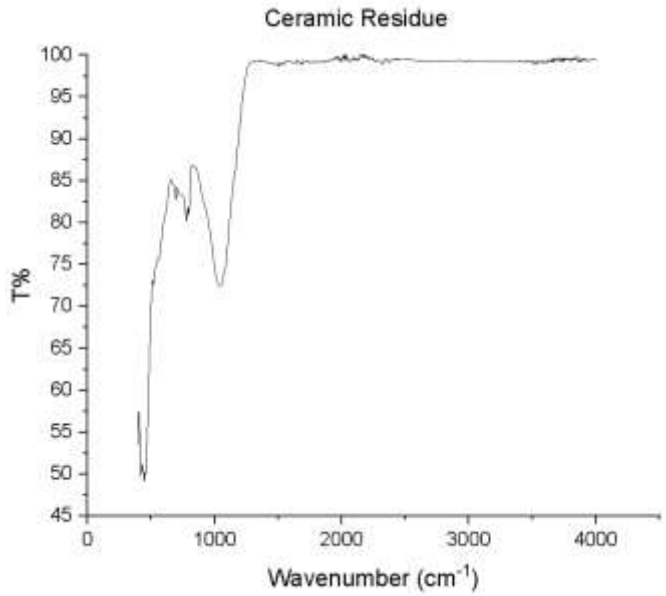

Figure 22 – FTIR analysis

2.6.4. Mechanical behavior

A single cylindrical specimen was produced to assess the mechanical resistance of the material. The quantity of material used for the paste is presented in Table 18. The activator used was hydroxide with a molar concentration of 5. The curing process of the paste is presented in Table 19. The specimen was successfully unmolded, has shown in Figure 23, and the mechanical results are presented in Table 20.

Table 18 – Paste quantities

Residue	Quantity (g)		S/L Ratio
	Precursor	Activator	
Ceramic Residue	100	35	0,35

Table 19 – Curing properties

Residue	Oven			Shelf		
	Temperature (°C)	Humidity (%)	Time (h)	Temperature (°C)	Humidity (%)	Time (h)
Ceramic Residue	80	0	47	20	60	48

Figure 23 – Ceramic residue specimen (after unmolding)

Table 20 – Mechanical results

Residue	Mechanical results	
	Compression (kN)	Compression (MPa)
Ceramic Residue	2,33	2,24

2.6.5. Leaching results

The leaching tests were conducted according to EN 12457-4. The results are as shown in Table 21.

Table 21 – Ceramic leaching results

Element	Concentration (ppm)	Limit values (ppm)		
		Inert	Non-hazardous	Hazardous
Cu	0,10±0,14	2	50	100
Zn	0,07±0,04	4	50	200
Pb	0,00±0,19	0,5	10	70
Cr	0,00±0,10	0,5	10	50
Chloride	15,69±1,69	800	15000	25000
Sulfate	59,26±4,53	1000	20000	50000

2.7. Plastic residue

Figure 24 illustrates the plastic residue after milling. This waste was only submitted to microstructural analysis, namely scanning electron microscopy, x-ray diffraction and Infra-red Spectroscopy, since its physical properties were considered irrelevant, as its specific role in the final composites was unclear, at the start of the study, and it was important to know its chemical and mineralogical composition, so that a possible research plan including this waste could be drawn. There was also no viable way of producing a specimen that could be tested for compressive strength, or any other type of mechanical performance, given the specific properties of plastic and, in particular, of the physical format (angular particles, with a wide size range) that this waste possessed.

Figure 24 - Photography of plastic residue after milling.

2.7.1. Composition

The composition of the plastic was defined through a XRD and MEV / EDS analysis. Table 22 and Figure 25 presents the results of EDS and XRD analysis, respectively.

Table 22 - EDS analysis

Elem	Wt %	At %	K-Ratio	Z	A	F
CK	48.10	71.99	0.0375	1.1154	0.0698	1.0000
OK	2.75	3.09	0.0041	1.0534	0.1406	1.0001

ClK	49.16	24.93	0.4444	0.8960	1.0090	1.0000
Total	100	100				

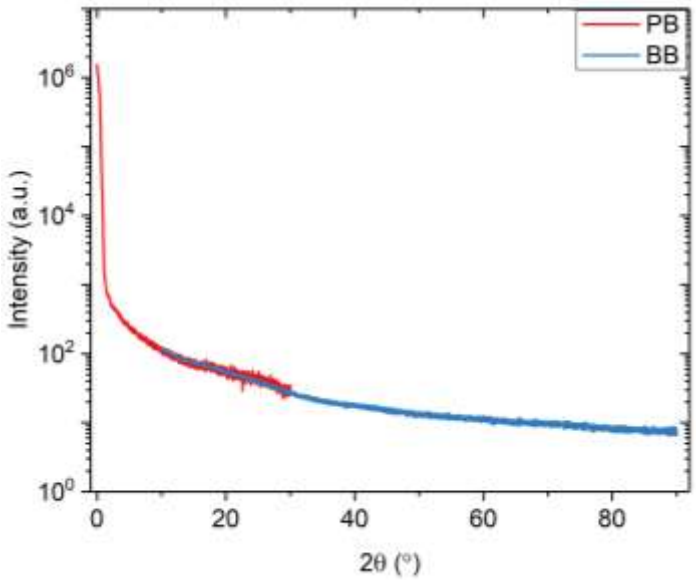

Figure 25 – XRD analysis.

Figure 26 presents the morphologic structure obtained using scanning electron microscopy, with magnification of 80 and 1000 times.

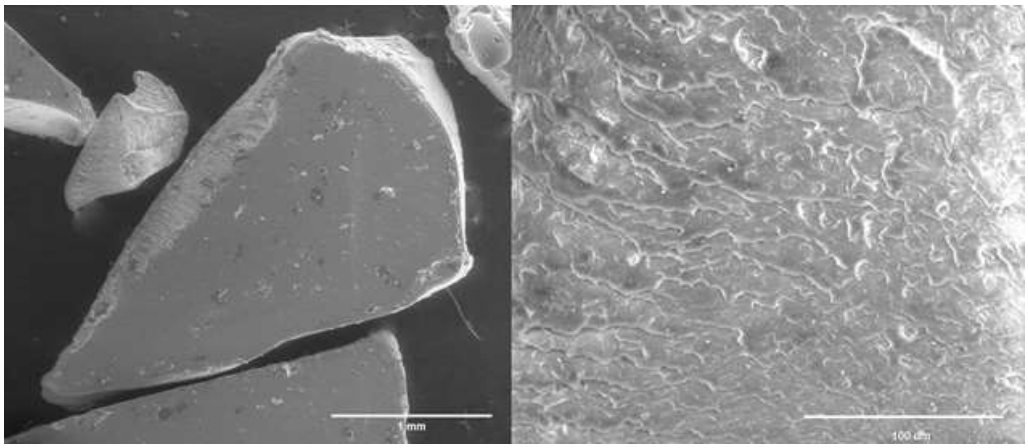

Figure 26 - SEM analysis

2.7.2. FTIR- ATR

Figure 27 presents the FTIR-ATR analysis of the three different colors of plastic (red, blue, and white) using a Perkin Elmer Spectrum BX equipment with frequency between 400 and 4000 cm^{-1} in transmission mode, resolution of 4 and 64 scans.

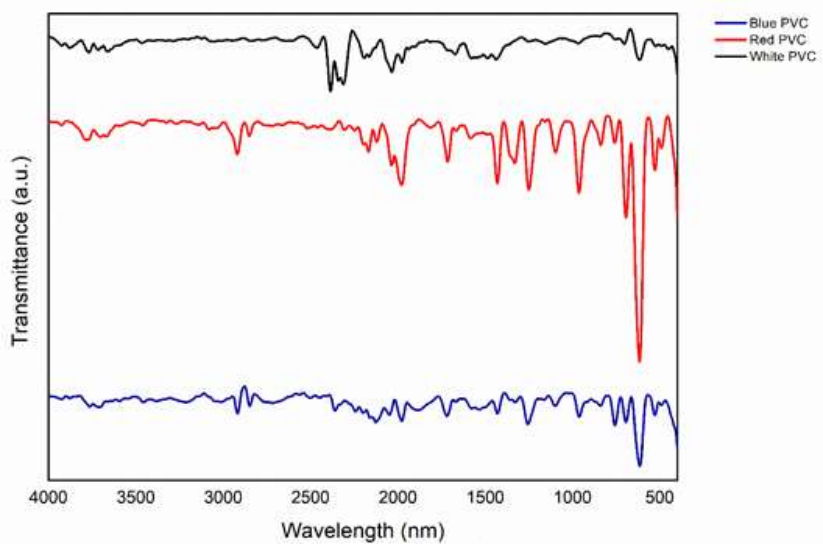

Figure 27 - FTIR analysis of plastics

2.8. Fly ash

2.8.1. Particle size distribution

Figure 28 presents the granulometry of the fly ash.

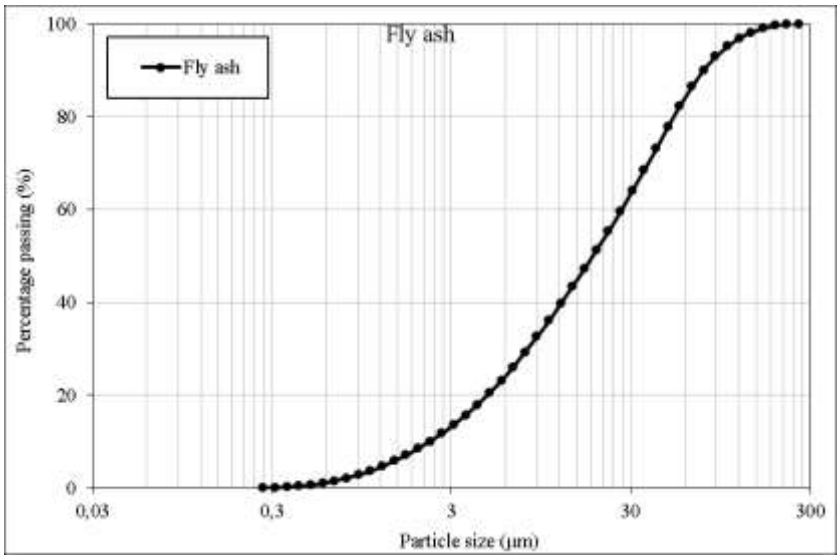

Figure 28 - Granulometry of the fly ash

2.8.2. Composition

The composition of the fly ash was obtained through XRD and XRF. The results are presented on Figure 29 and Table 23, respectively.

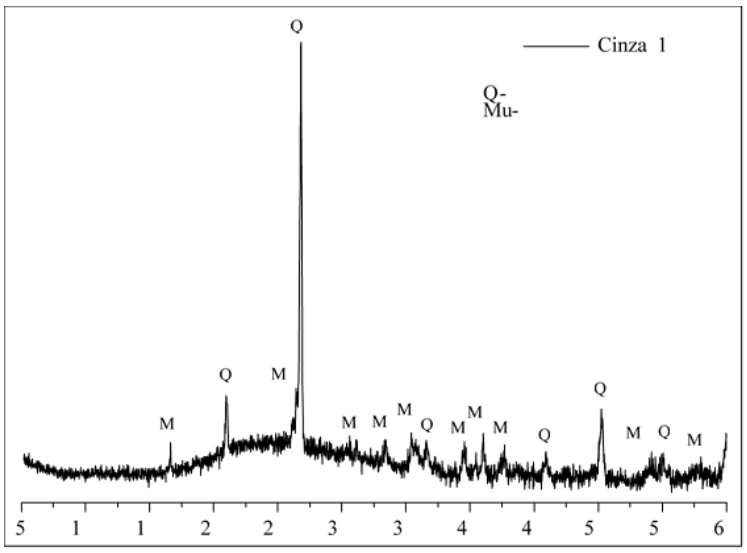

Figure 29 - XRD analysis

Table 23 - XRF analysis

Element	%

Al2O3	21,44
BaO	0,13
CaO	1,31
Cr2O3	0,06
Fe2O3	8,20
Ga2O3	0,01
K2O	2,81
MgO	1,46
MnO	0,07
Na2O	1,12
P2O5	0,24
Rb2O	0,01
SiO2	56,11
SO3	0,66
SrO	0,04
TiO2	1,15
ZnO	0,03
ZrO2	0,10
L.O.I.	5,05

2.8.3. FTIR

Figure 30 presents the FTIR analysis of the fly ash using a Shimadzu IRAffinity-1S equipment with wave range between 400 and 4000 cm^{-1}, resolution of 4 and 64 scans.

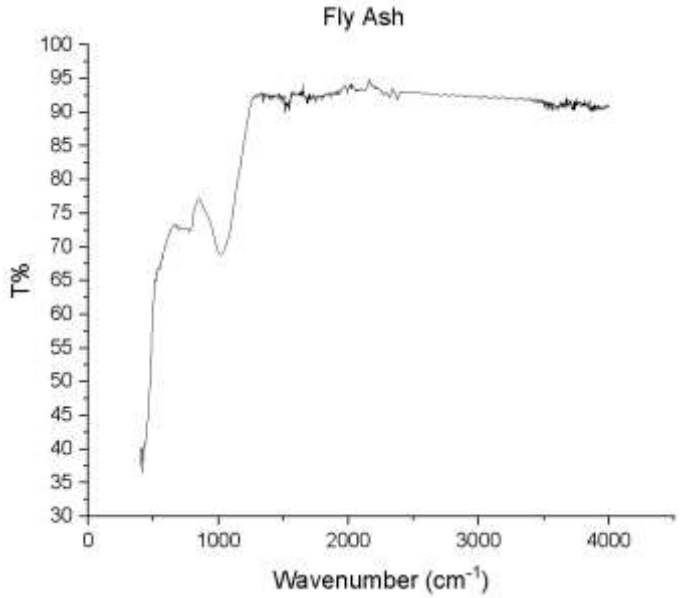

Figure 30 – FTIR analysis

2.8.4. Mechanical behavior

A single cylindrical specimen was produced to assess the mechanical resistance of the material. The quantity of material used for the paste is presented in Table 24. The activator used was hydroxide with a molar concentration of 5. The curing process of the paste is presented in Table 25. The specimen was successfully unmolded, has shown in Figure 31, and the mechanical results are presented in Table 26.

Table 24 – Paste quantities

Residue	Quantity (g)		S/L Ratio
	Precursor	Activator	
Fly Ash Residue	140	60	0,43

Table 25 – Curing properties

Residue	Oven		
	Temperature (°C)	Humidity (%)	Time (h)
Fly Ash Residue	85	40	22

Figure 31 – Fly ash residue specimen (after unmolding)

Table 26 – Mechanical results

Residue	Mechanical results	
	Compression (kN)	Compression (MPa)
Fly ash Residue	0,95	0,90

2.8.5. Leaching results

The leaching tests were conducted according to EN 12457-4. The results are as shown in Table 27.

Table 27 – Fly ash leaching results

Element	Concentration (ppm)	Limit values (ppm)		
		Inert	Non-hazardous	Hazardous
Cu	0,00±0,14	2	50	100
Zn	0,02±0,04	4	50	200
Pb	0,00±0,19	0,5	10	70
Cr	0,02±0,09	0,5	10	50
Chloride	8,73±1,67	800	15000	25000
Sulfate	32,26±3,41	1000	20000	50000

2.9. Marble residue

Given the state of the material on arrival, the residue was dried and sieved using 2,0mm and 500µm sieves. This process allowed the disaggregation of the bigger particles and the removal of small metal fragments from the marble cutting process. The result of the initial treatment is presented in Figure 32.

Figure 32 - Marble residue before (a) and after (b) sieving

2.9.1. Composition

The composition of the marble residue was obtained through SEM, EDS and XRD analysis, presented on Figure 33, Table 28 and Figure 34, respectively.

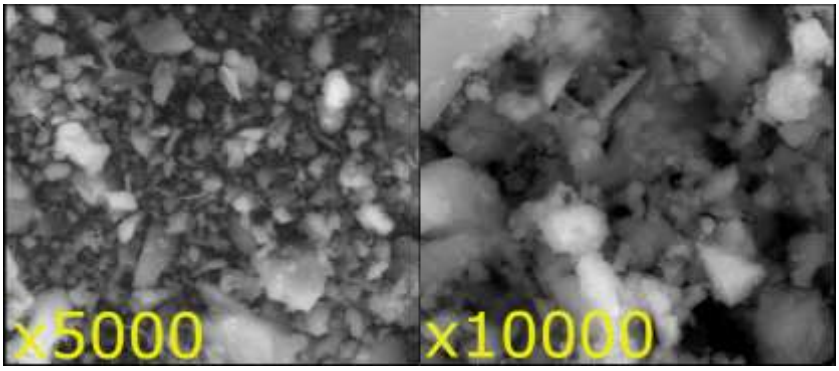

Figure 33 – SEM analysis

Table 28 – EDS analysis

Element (%)	Ponto				
	1	2	3	4	5
Na	3,73	4,31	3,87	3,60	3,95
Mg	1,53	1,14	1,31	1,75	1,43
Al	10,51	10,61	10,83	10,75	10,55
Si	47,25	47,03	45,74	45,81	47,25
P	-	-	0,70	0,89	1,17
K	5,18	4,73	4,79	4,78	5,07
Ca	30,75	31,37	31,71	31,58	29,47
Fe	0,83	0,81	0,81	0,84	0,82
Cu	0,22	-	0,23	-	0,27

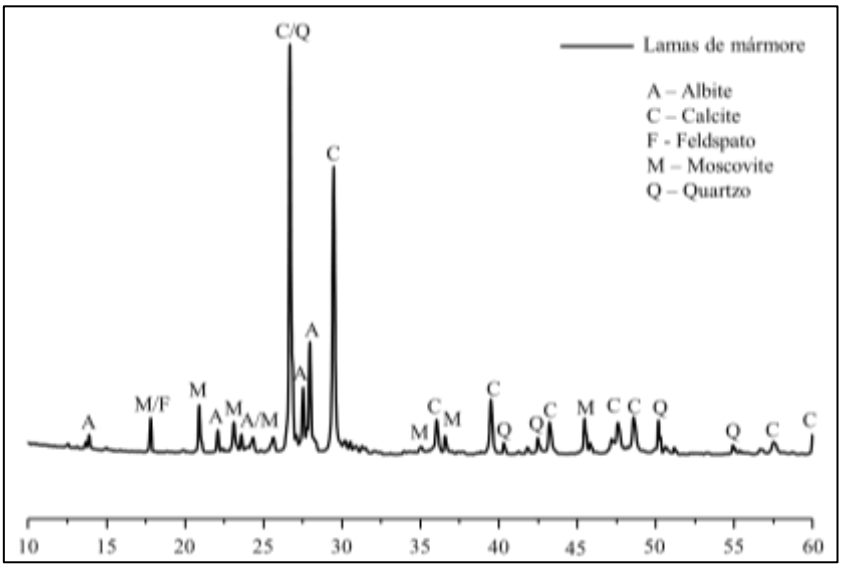

Figure 34 – XRD analysis

2.9.2. FTIR

Figure 35 presents the results of FTIR analysis using a Shimadzu IRAffinity-1S equipment with wave range between 400 and 4000 cm^{-1}, resolution of 4 and 64 scans.

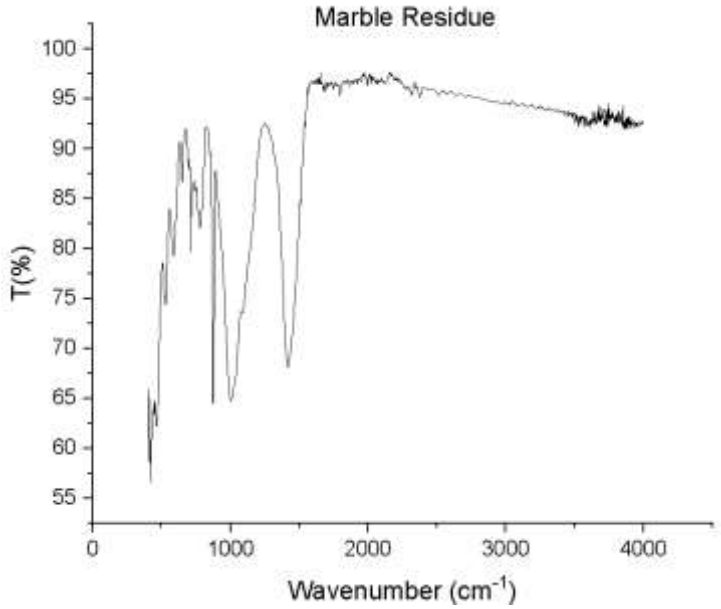

Figure 35 – FTIR analysis

2.9.3. Mechanical behavior

A single cylindrical specimen was produced to assess the mechanical resistance of the material. The quantity of material used for the paste is presented in Table 29. The activator used was hydroxide with a molar concentration of 5. The curing process of the paste is presented in Table 30. The specimen was successfully unmolded, has shown in Figure 36, and the mechanical results are presented in Table 31.

Table 29 – Paste quantities

Residue	Quantity (g)		S/L Ratio
	Precursor	Activator	
Marble Residue	80	39	0,49

Table 30 – Curing properties

Residue	Oven		
	Temperature (°C)	Humidity (%)	Time (h)
Marble Residue	85	40	22

Figure 36 – Marble residue specimen (after unmolding)

Table 31 – Mechanical results

Residue	Mechanical results	
	Compression (kN)	Compression (MPa)
Marble Residue	1,84	1,79

2.9.4. Leaching results

The leaching tests were conducted according to EN 12457-4. The results are as shown in Table 32.

Table 32 – Marble leaching results

Element	Concentration (ppm)	Limit values (ppm)		
		Inert	Non-hazardous	Hazardous
Cu	0,03±0,14	2	50	100
Zn	0,02±0,04	4	50	200
Pb	0,00±0,19	0,5	10	70
Cr	0,00±0,10	0,5	10	50
Chloride	5,52±1,70	800	15000	25000
Sulfate	12,98±3,31	1000	20000	50000

2.10. Granite residue

Given the state of the material on arrival, the residue was dried and sieved using 2,0mm and 500µm sieves. This process allowed the disaggregation of the bigger particles and the removal of small metal fragments from the marble cutting process. The result of the initial treatment is presented in Figure 37.

Figure 37 - Granite residue before (a) and after (b) sieving

2.10.1. Composition

The composition of the granite residue was obtained through SEM, EDS and XRD analysis, presented on Figure 38, Table 33 and Figure 39, respectively

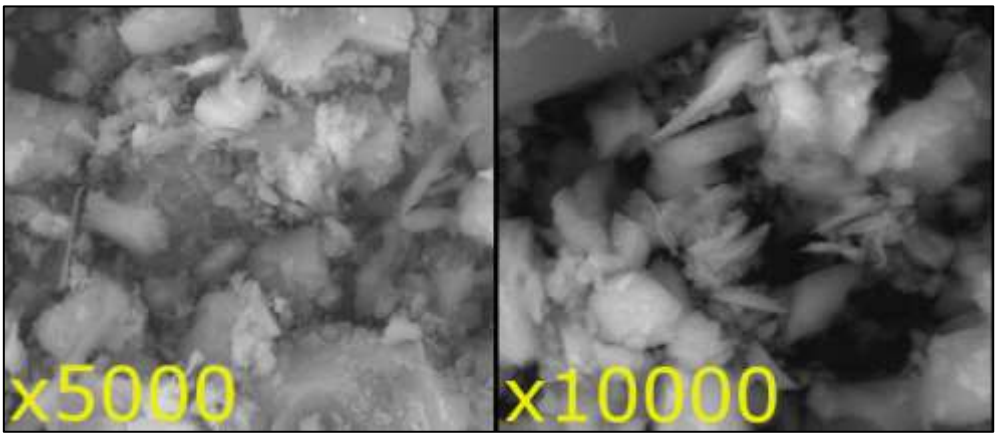

Figure 38 - SEM analysis

Table 33 - EDS

Element (%)	Ponto				
	1	2	3	4	5
Na	4,81	4,66	4,50	4,82	4,83
Mg	1,10	1,12	0,67	0,99	0,66

Al	14,01	13,18	12,33	12,73	12,21
Si	67,69	67,24	68,47	66,83	68,31
K	7,82	8,38	9,06	8,92	8,80
Ca	3,38	3,72	3,64	4,24	3,75
Fe	1,19	1,70	1,33	1,47	1,44

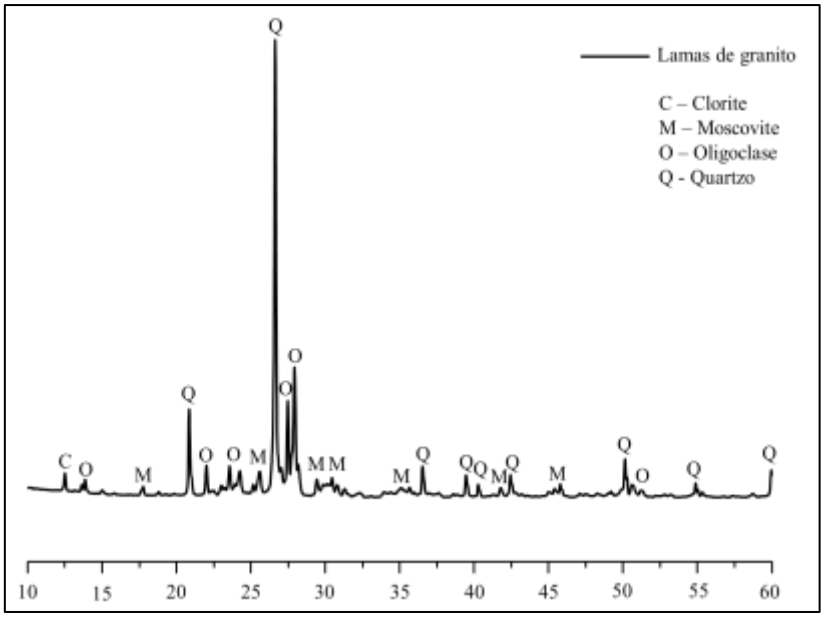

Figure 39 – XRD analysis

2.10.2. FTIR

Figure 40 presents the results of the FTIR analysis using a Shimadzu IRAffinity-1S equipment with wave range between 400 and 4000 cm^{-1}, resolution of 4 and 64 scans.

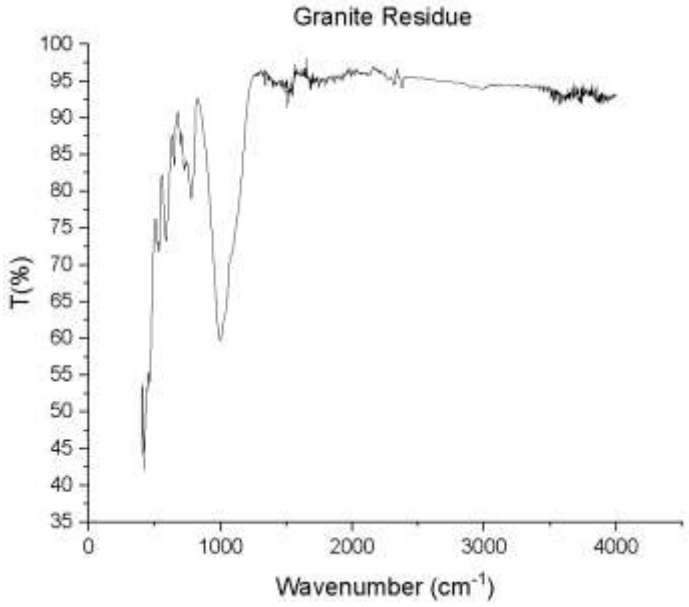

Figure 40 – FTIR analysis

2.10.3. Mechanical behavior

A single cylindrical specimen was produced to assess the mechanical resistance of the material. The quantity of material used for the paste is presented in Table 34. The activator used was hydroxide with a molar concentration of 5. The curing process of the paste is presented in Table 35. The specimen was successfully unmolded, has shown in Figure 41, and the mechanical results are presented in Table 36.

Table 34 – Paste quantities

Residue	Quantity (g)		S/L Ratio
	Precursor	Activator	
Granite Residue	80	48	0,60

Table 35 – Curing properties

Residue	Oven		
	Temperature (°C)	Humidity (%)	Time (h)
Granite Residue	85	40	22

Figure 41 – Granite residue specimen (after unmolding)

Table 36 – Mechanical results

Residue	Mechanical results	
	Compression (kN)	Compression (MPa)
Granite Residue	0,20	0,20

2.10.4. Leaching results

The leaching tests were conducted according to EN 12457-4. The results are as shown in Table 37.

Table 37 – Granite leaching results

Element	Concentration (ppm)	Limit values (ppm)		
		Inert	Non-hazardous	Hazardous
Cu	0,15±0,14	2	50	100
Zn	0,05±0,04	4	50	200
Pb	0,00±0,19	0,5	10	70
Cr	0,05±0,09	0,5	10	50
Chloride	5,34±1,71	800	15000	25000
Sulfate	8,52±3,39	1000	20000	50000